Egypt. J. Chem. Vol. 67, SI: M. R. Mahran, pp. **2101 - 2106** (2024)

Egyptian Journal of Chemistry

http://ejchem.journals.ekb.eg/

S-limonene loaded gum Arabic nanoparticles ameliorates wound healing and inhibits herpes simplex virus.

Habiba A. Ahmed[1,2*] , Zeinab A. Salama[1] and Amr A. Nassrallah[3,4]

[1] *Plant Biochemistry Department, National Research Centre, 12622 Dokki, Giza, Egypt.*

[2] *Medical Biotechnology Department, Genetic Engineering and Biotechnology Research Institute, City of Scientific Research and Technological Applications, New Borg El-Arab City, Alexandria 21934, Egypt.*

[3] *Basic Applied Science institute, Egypt-Japan University of* Science *and Technology (*E-JUST*), New Borg El-Arab City, Alexandria 21934, Egypt.*

[4] *Biochemistry Department, Cairo University Research Park, Cairo University, 12613 Giza, Egypt*

Abstract

Essential oils are composed of mixture of compounds that display wide industrial, pharmaceutical and cosmetics applications singularly or in combination, including food preservation, diseases treatment and antimicrobial agents. In this study, S-limonene was subjected to nanofabrication using Gum Arabic and tested for their potential wound healing against Bj-1 fibroblast normal cell line. The physical properties of the new formula exhibited nano-characteristics based on morphological properties using TEM imaging, size using zeta sizer and linkage between gum Arabic polymer and s-limonene using FTIR analysis. The results of wound healing activity were measured via cell migration assay of scratched monolayer Bj-1 cell. In this context, both the S-limonene and S-limonene-GA-NPs exhibited potential wound repair compared to Gum Arabic GA-NPs control. In addition, the immunoblotting of collagen type III and Matrix Metalloproteinase MMP-2 and MMP-9 showed an accumulation of Collagen III protein level. Moreover, a slight increase in the MMP-2 and MMP-9 protein levels. These results indicated that S-Limonene-GA-NPs illustrate healing properties against Bj-1 fibroblast cell wound closure after 24 h followed by s-limonene, while no significant effect of Gum Arabic-NPs were detected compared to control. In conclusion, the preparation of s-limonene nanoparticles by covering them with gum Arabic showed biological activity as an anti-viral agent and wound healing potential. As well as S-limonene-and its nanoform was tested for the anti-herbal virus HSV-1 and HSV-2 as well as wound healing properties of nano-formulated S-limonene loaded with gum Arabic. S-Limonene-NPs exhibited antiviral activity against HSV-1 and HSV-2 with 73.3 and 56.6 %, respectively followed by native s-limonene with 46.6 and 40%, respectively. However, slightly antiviral properties were observed due to gum Arabic-NPs treatment of HSV-1 and HSV-2 with 6.6 and 3.3%, respectively.

Key words: S-limonene, nanoparticles, gum Arabic, wound healing, and antiviral activity.

.

1. Introduction

The Citrus Gum Arabic is a polysaccharide abundant in Acacia species [1]. It is widely used as an emulsifier in food additives and medicinal applications to stabilize processing. In addition, it is known to have therapeutic properties for various diseases such as high blood pressure, diabetes mellitus, and stroke [1]. Furthermore, the most studied illustrated that it has a vigorous antioxidant potential [2]. The essential oils of citrus fruits peels (Rutaceae) are rich in d-limonene, which is a monoterpene. Many studies showed that the limonene has anti-inflammatory potential anxiolytic, anti-nociceptive and antioxidant activity [3-7]. Herpes simplex virus (HSV) is a pathogenic virus for humans, which divided into two types: type one is HSV-1 infections is prevalent and especially influences adult people and type two is HSV-2 [8]. HSV proliferates and infects the mucocutaneous surface at the place of entry cells. Moreover, repeated infections with some patients due to the inherent virus being spontaneously reactivating. Therefore, antiviral medications such as valacyclovir, famciclovir and acyclovir can be used to inhibit the virus or reduce the course and lower the riskiness of clinical symptoms [9]. On the other hand, some antiviral medications exhibited toxic side effects and the viral progress made resistance towards these antiviral medications. For those reasons, the need to discover new compounds as antiviral agents is a challenge. In addition, different essential oils from various plants have a good source as wound healing potential [10&11]. Therefore, in this study, the formulation of s-limonene nanoparticles was carried out for optimizing the physical stability of s-limonene by coating it with gum Arabic and was determined the biological activity as anti-viral agent and wound healing potential of them.

MATERIALS AND METHODS

In this study, all chemicals used were purchased from Sigma (USA) and Fluka (Switzerland) at analytical grade.

Preparation of nanoparticles:

Freeze drying method utilized to synthesize s-limonene NPs with some modifications [12]. Initially, dissolving 6 ml of s-limonene and 2 ml tween 80 in 60 mL deionized water containing 20 gm. of gum Arabic. The previous mixture was melding agitation for 72 h at room temperature. Using DAIGGER ULTRA-SONIC Model GEX 750, USA to sonicate the mixture for 20 min. Then, the product freeze-dried at -55 °C for 24 h. The

*Corresponding author e-mail: amr.nassrallah@ejust.edu.eg (Amr A. Nassrallah)

Receive Date: 18 September 2024, Revise Date: 03 November 2024, Accept Date: 24 November 2024

DOI: 10.21608/ejchem.2024.322144.10458

final product was sifted (stainless-steel sieve 230 mesh) and stored at -20 °C in airtight container until use.

Physical characterization:

After 24 hours, nanoparticles, including gum Arabic-Nanoparticle (GA-NP) or S-limonene- gum Arabic-Nanoparticle (S-limonene-GA-NP) suspended in 10 mL of distilled water, and then filtered using filter paper (Whatman NO1). The previous suspension of NPs was analyzed (zeta potential values, the NPs dimension and polydispersity index PDI) using Nano- ZS, Malvern instruments Ltd.,UK. The association degree between substances of nanoparticles evaluated using FTIR (Fourier transform infrared spectroscopy VERTEX 80v, BRUKER, Germany), the scale range was 4000-400 cm^{-1}, and the resolution was 4 cm^{-1}. Transmission electron microscope TEM (JEM 2100 HRT, HIGH RESOLUION MADE IN JAPAN) was used to evaluate the morphology of nanoparticles of gum Arabic and s-limonene [13,14,15,16].

Wound Healing Assay

The wound healing properties of S-limonene, S-limonene-GA-NPs and GA-NPs on Bj-1 fibroblast cells were evaluated by the potential migration ability of wound-induced scratch assay. The BJ-1 cells were seeded at 1 × 10^6 cells/well into fibronectin-coated eight well plates. The cells monolayer was manually scratched with a yellow PBS-rinsed plastic pipette tip and treated with 0, 5, 10, 25 and 50 ng/ml solution of different samples dissolved in DMEM, or only with DMEM as control. The two-dimensional cell migration was determined by imaged using inverted microscope equipped with a digital camera. Wound closure was measured by wound area at 0 time and 24 h[14].

Western blot analysis

Western blot analyses of wound healing involved proteins including Collagen III, MMP-2 and MMP-9 were conducted as previously described by [15]. Scratched Bj-1 fibroblast normal cells exposed to S-Limonene, S-Limonene-GA-NPs and GA-NPs with 50 ng/ml. After 48h cells were collected and homogenized in extraction buffer containing 150 mM NaCl, 50 mM Tris-HCl pH 7.5, 10 mM $MgCl_2$, 1 mM PMSF, 0.1 % NP-40 and 1x complete protease inhibitor (Roche. Extracts were clarified two times by centrifugation at 13000 x g during 10 min at 4 °C. The cell homogenate was clarified twice by centrifugation at 14000 rpm/ 10 min, and supernatant was transferred to a new tube and the protein content was quantified by the Bradford protein assay method (Bio-Rad®). Twenty µg of protein extract were heated at 95 °C for denaturation for 5 min in 2x loading buffer and separated in 12% SDS-PAGE gels depending on the target protein size. The gels were transferred to a PVDF membrane using semidry transfer blot system. They were then saturated with 5% non-fat milk diluted in PBS buffer 0.1% Tween-20 (PBS-T) and used for immunodetection with the anti-collagen type III monoclonal antibody (PAb 240; ab26; Abcam UK), anti-MMP2 monoclonal antibody (E17; ab32124; Abcam UK), anti-MPP9 monoclonal antibody (E63, ab32503; Abcam UK), antibodies. The secondary antibodies used were: Anti-Mouse IgG (Amersham Biosciences, Buckinghamshire UK) and Anti-Rabbit (GE Healthcare, Milwaukee, WI, United States).

Antiviral potential.

Cytotoxicity test

In brief, dissolving 100 mg of samples (Gum arabic, s-limonene, and s-limonene-NPs) in 1 ml of solvent. Then, add 24 µL of 100X of antibiotic–antimycotic mixture to 1 ml of the sample to protect it from contamination. To determine nontoxic dose of the tested samples: bi-fold dilutions were done to 100 µl then adding 100 µl of the original dissolved sample and 100 µl of each dilution was inoculated in an African green monkey kidney cell line (Vero) (obtained from the Holding Company for Biological Products & Vaccines VACSERA, Egypt) previously cultured in 96 multi-well plates (Greiner-Bio one, Germany). The morphology evaluation of cells was estimated using inverted light microscope and trypan blue test[15&16].

Cell morphology changes.

Initially, seeding of vero cells (2×10^5 cells/ml) onto culture plate (96-well). After incubation for 24 h at 37° C in 5% (v/v) CO_2, the medium culture was removed and replenished with 100 µl of bi-fold dilutions of the sample tested prepared in DMEM (GIBCO BRL). After incubation for 3 days in 5% CO_2 at 37°C, cell morphology was observed daily under the microscope and morphological changes were scored [15].

Cell viability assay

The same assay described above for tested samples but, after incubation for 3 days the medium was removed, cells were trypsinized and an equal volume of 0.4% (w/v) trypan blue dye aqueous solution was added to cell suspension. Viable cells were counted under phase contrast microscope [16].

Determination of Herpes simplex virus type 1 and 2 (Titers Using plaque assay)

Non-toxic dilutions were mixed (100 µl) with 100 µl of different doses of herpes simplex virus type 1 and 2 (HSV-1and HSV-2) ($1X10^5$, $1X10^6$, $1X10^7$) Plaque-Forming Units per milliliter (PFU/ml). The mixture was incubated for 1/2 hr at 37°C. The inoculation of (100 µl) 10-fold dilutions of treated and untreated HSV-1and HSV-2 was carried out separately into Vero cell line in 12 multi well-plates. After 1 hr of incubation for adsorption at 37°C in a 5% CO2-water vapor atmosphere without constant rocking. The plates were rocked intermittently to keep the cells from drying. After adsorption, 1 ml of 2X media (Dulbecco´s Modified Eagle Medium, Gibco- BRL (DMEM) plus 1ml 1% agarose was added to each well and the plates were incubated at 37°C in a 5% CO2-water vapor atmosphere. After the appropriate incubation period, the cells were stained with 0.4% crystal violet after formaline fixation, and the number of plaques were counted. The viral titers were then calculated and expressed as PFU/ml [17]. Statistics: Mean and standard deviation were calculated.

RESULTS AND DISCUSSION

Physical characterization of nanoparticles

Particle size distribution.

To characterize the formulated s-limonene loaded Gum Arabic, Particle size (nm), particles surface charge (zeta potential mV) and Polydispersity index (PDI) are shown in Table 1. The results illustrated that particle size of S-limonene was less than 100 nanometers with expected size

of 12.8 nm, indicated that particles were in nano scale. In addition, the surface charge of particles was negative -17.6 mv which attributed to slow flocculation or coagulation. The PDI value of nanoparticles was 0.35 indicated that the significant high diffusion rate into hydrophilic solutions [18].

Table 1. Particle size, Polydispersity index (PDI) and Zeta potential of s-limonene–NPs and gum Arabic-NPs.

	s-limonene-NPs	Gum arabic-NPs
Partial size (nm)	12.08	6.10
Pdi	0.35	0.66
Zeta potential (mV)	-17.60	-9.19

Fourier-transform infrared spectroscopy (FTIR)

The FTIR spectrum of s-limonene (blue), gum Arabic (black) and s-limonene-NPs (red) was shown in Figure 1. In general, the spectrum of s-limonene displayed an absorbed bands at 989 and 890 cm^{-1} corresponds to C-H. In addition, a band at 3001 cm^{-1} corresponds to = C-H and the band at 1677 cm^{-1} corresponds to C=C. The –CH linkage appeared at 2855, 2913, and 2962 cm^{-1}. The absorption peak at 1644 cm^{-1} is attributed to C=C [19]. However, Gum Arabic spectrum illustrated different significant bands at 3339 cm^{-1} corresponds to -OH, 2881 cm^{-1} corresponds to -CH_2 and 1607 cm^{-1} corresponds to -C-O. As well as other bands at 1404 cm^{-1} correspond to –CH and at 1062 cm^{-1} assigned to C–O–C and the band at 610 cm^{-1} indicated to –C–H linkage [20]. The spectrum of s-limonene-NPs exhibited high overlapped between at all described beaks of s- limonene and gum Arabic, respectively. In addition, a new inducted band at 1726 cm^{-1} Figure 1. These results indicated solid interaction and high linkage between s-limonene and gum Arabic.

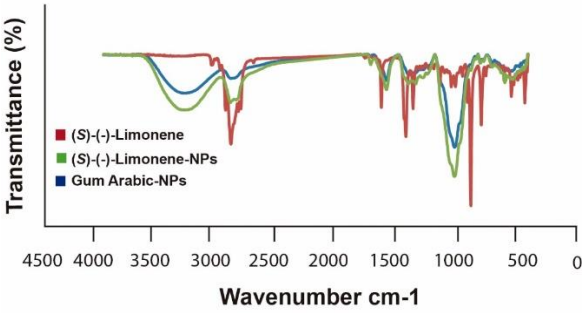

Figure 1. Fourier-transform infrared spectroscopy (FTIR) spectra of gum Arabic-NPs (blue), s-limonene (Red) and s-limonene–NPs (green).

Transmission Electron Microscope TEM.

The morphology and size distribution of s-limonene-GA-NPs in comparison GA-NPs were subjected to TEM analysis Figure 2. The results showed that the clear layer on the surface of gum Arabic nanoparticles (Figure 2A and B). This layer is due to a binding between s-limonene and gum Arabic for increasing stability of s-limonene. TEM images of prepared gum Arabic nanoparticles in the range 2.6 – 5.8 nm (Figure 2B) compared to gum Arabic loaded s-limonene nanoparticles in the range of approximately 10–30 nm (Figure 2B). However, the results showed an increase of particle size formation compared to the results of zeta sizer may be due to the larger viscosity of the dispersed phase during ultra-sonication [21].

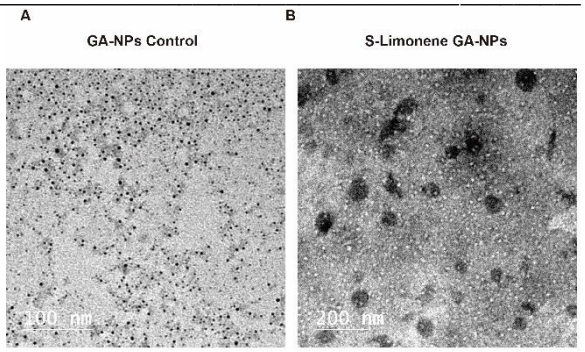

Figure 2. Transmission electron microscope micrographs of gum Arabic-NPs (A) and s-limonene-NPs. (B).

Wound Healing potential

To assessment the wound healing potential activity, a confluent monolayer Bj-1 normal fibroblast into 12 well plate was artificial scratching and subjected to s-limonene, s-limonene-GA-NPs and GA-NPs treatment with different concentration of 5, 10, 25 and 50 ng/ml (data not showed). After 48 h the cell movement was measured by microscopic imaging of cell migration. The results indicated that both S-limonene and its Nano form showed potential wound healing activity at 50 ng/ml Figure 3. Surprisingly, s-limonene GA-NPs displayed significantly higher potential wound healing activity compared to s-limonene. No significant wound healing activity was observed due to Gum Arabic-NPs treatment. Wound healing is a systematized and complex process that requires different types of cells and series of interactions with cytokines, growth factors, and soluble mediators, for repair of wounded tissue. Cutaneous fibroblasts are the basic line of protection and response to scratch and are necessary for dermal damage repair. The fibroblasts show in the scratch site after injury, through the inflammatory stage, reproduce and synthesize growth factors. In addition, in the phase of granulation tissue formation the new extracellular matrixes appear and then produce mechanical power during the wound to begin wound constriction[22]. Recently, the traditional medicinal plant confirmed for the therapy of minor wounds and inflammation of the skin. Monoterpenes are organic compounds with different therapeutic potential and biological activities. Using this terpene (s-limonene) exhibited a stimulatory impact on fibroblast generation and wound healing process[23]. In recent years, extensive studies were carried out on the role of citrus essential oils as wound healing activity [24-26]. In this context AgNPs loaded Citrus lemon displayed significant wound healing properties [27]. Moreover, d-limonene, the most abundant terpene in Limone essential oil 40% exhibited skin lesions repair activity [28].

Western blot of wound healing related proteins

The mode of action of potential wound healing activity was also determined by immunoblotting of wound healing target markers. Results of immunoblotting analysis, using anti-Collagen III, anti-MMP-2, anti-MMP-9 antibodies, indicated a significant increase of accumulation of Collagen III in Bj-1 cells exposed to 50 ng/mL of S-limonene and S-limonene-NPs compared to GA-NPs relative to untreated cells **Figure 4**. In addition, MMP-2 and MPP-9 protein levels were slightly increased in wounded cells after 48 h of S-Limonene-GA-NPs treatment. However, the treatment resulted in significant

accumulation in the Protein levels of the wound healing marker were higher in cells treated with s-limonene-NPs compared to L-limonene (**Figure 4**).

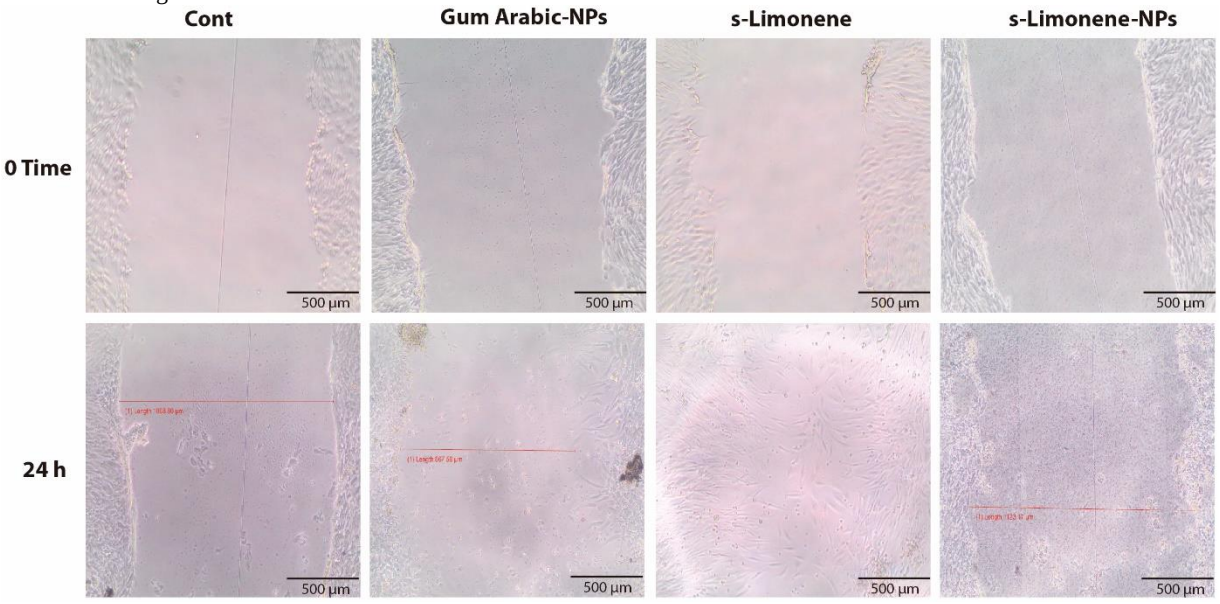

Figure 3. Effects of gum Arabic-NPs, s-limonene, and s-limonene-NPs on migration changes in BJ-1 fibroblast cells after treatment monitored by phase contrast microscopy at zero time and after 24 h.

Several Studies revealed that MMPs involved in epithelial cells developed at different levels including inflammatory stage which is also the initial stage of wound healing [29,30]. In this context, MMP-2 and MMP-9 proteins displayed a potential therapeutic role in wound healing via stimulating the pro-inflammatory markers. It has been reported that alteration of MMP-2 expression level might play a role in cell–cell interactions inducing an inflammatory status that is associated with wound healing[31].

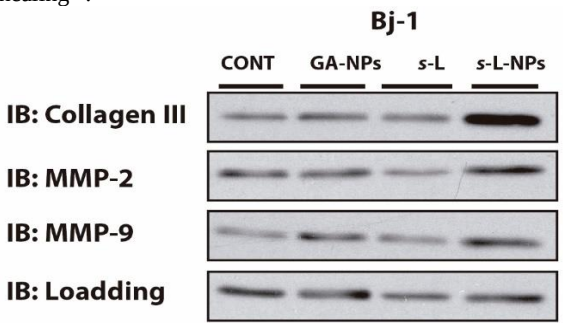

Figure 4. Immunoblotting of wound healing related markers of Bj-1 cells treated with S-limonene and S-limonene-GA-NPs.

Antiviral potential.

In the current study, the antiviral activity of s-limonene, s-limonene-NPs and GA-NPs against infection of herpes simplex HSV1 and HSV2 virus was examined. The results showed that S-Limonene-GA-NPs displayed the highest antivirus activity against HSV1 with 73.3%, followed by S-limonene with 46.6%. However, GA-NPs showed the lowest activity against HSV1 virus with 6.6% Figure 5. Similarly, S-Limonene-GA-NPs exhibited the highest antiviral activity against HSV-2 followed by S-limonene and GA-NPs. However, the activity against HSV-2 was lower with antiviral activity of 56.6%, 40% and 3.3%, respectively Figure 5. No cytotoxic activity was detected on the Vero cells Table 2. We expected that S-limonene is targeting virus proteins or due to the high ability to penetrate the virus. In addition, the nano-formulation of S-limonene enhances the efficacy against viruses due to altered physical properties. However, the mode of action as antivirus requires further investigation. The inhibition of viral activity due to binding of the bioactive compounds to viral proteins, whether the viral penetration or adsorption on the host cells [32]. On the other hand, the antiviral drug such as acyclovir effect on the replication of virus by interference with the DNA polymerase inside the cell [33]. Results of non-toxic doses of examined materials on Vero cell line are shown in Table 2.

Table 2: Non-toxic doses of tested materials on different cell lines (µg)

Samples	Vero
S-Limonene NPs	80
Control	90
S-Limonene	Dilution 1/1000

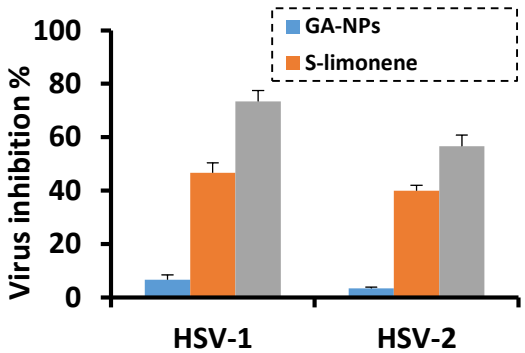

Figure 5. Antiviral activity of HSV-1 and HSV-2 treated with S-limonene and S-limonene-GA-NPs.

CONCLUSION

In this study, we utilized TEM, zeta potential, and FT-IR methods to characterize the produced nanoparticles. The FT-IR spectra revealed a significant interaction between Gum Arabic and S-limonene. TEM imaging indicated that the size of S-limonene nanoparticles was approximately 30 nm. The data strongly suggest that S-limonene exhibits wound healing properties and offers protection against skin damage through enhanced cell migration in scratched Bj-1 fibroblast cell monolayers, along with increased levels of Matrix Metalloproteinases (MMPs) MMP-2 and MMP-9, as well as Collagen III proteins (Figure 2A and B).

Furthermore, the nano-formulation of S-limonene enhances efficacy by altering various physical properties, including size, shape, and delivery mechanisms. Notably, S-limonene and S-limonene-GA-NPs demonstrated significant inhibitory effects against herpes simplex virus infections. Our findings indicate that S-limonene-GA-NPs exhibited the highest antiviral activity against both HSV-1 and HSV-2, surpassing that of the native form of S-limonene. These results suggest that essential oil monoterpenes like S-limonene possess potent anti-herpetic activities early in the viral replication cycle, indicating their potential as antiviral therapeutics.

In summary, our findings underscore the multifaceted benefits of S-limonene, particularly its anti-inflammatory and wound-healing properties. The ability of S-limonene to reduce inflammation and neo-angiogenesis highlights its direct effects on epithelial cells, suggesting promising applications in both dermatological treatments and antiviral strategies. This study opens avenues for further exploration of S-limonene and its derivatives in the development of innovative therapeutic agents aimed at enhancing skin repair and combating viral infections.

Declarations

Ethics approval and consent to participate.

This experiment does not involve human experiments and animal experiments. All methods were performed in accordance with the relevant guidelines and regulations.

Consent for publication

Not applicable

Availability of data and materials

All data generated or analyzed during this study are included in this published article.

Competing interests

The authors declare that they have no competing interests.

Funding

The authors declare that they have no funding role in the design of the study; in the collection, analyses, or interpretation of data; in the writing of the manuscript, or in the decision to publish the results.

Author contributions

HAA, ZAS and AAN designed the experiments. HAA and AAN performed the experiments and data analysis and drafted the manuscript. All authors read and prepare the final manuscript.

Acknowledgements

Not applicable.

References

1. Ali, B. H., Ziada, A., Al Husseni, I., Beegam, S., Al-Ruqaishi, B., & Nemmar, A. (2011). Effect of Acacia gum on blood pressure in rats with adenine-induced chronic renal failure. *Phytomedicine*, 18(13), 1176-1180.
2. Kong, H., Yang, J., Zhang, Y., Fang, Y., Nishinari, K., & Phillips, G. O. (2014). Synthesis and antioxidant properties of gum arabic-stabilized selenium nanoparticles. *International Journal of Biological Macromolecules*, 65, 155-162.
3. Ahmed, H. A., Nassrallah, A. A., Abdel-Raheem, M. A., & Elbehery, H. H. (2023). Lemon peel essential oil and its nano-formulation to control *Agrotis ipsilon* (Lepidoptera: Noctuidae). *Scientific Reports*, 13(1), 17922.
4. Piccinelli, A. C., Morato, P. N., dos Santos Barbosa, M., Croda, J., Sampson, J., Kong, X., & Kassuya, C. A. L. (2017). Limonene reduces hyperalgesia induced by gp120 and cytokines by modulation of IL-1β and protein expression in the spinal cord of mice. *Life Sciences*, 174, 28-34.
5. Roberto, D., Micucci, P., Sebastian, T., Graciela, F., & Anesini, C. (2010). Antioxidant activity of limonene on normal murine lymphocytes: Relation to H_2O_2 modulation and cell proliferation. *Basic & Clinical Pharmacology & Toxicology*, 106(1), 38-44.
6. Al Kamaly, O., Numan, O., Almrfadi, O. M., Alanazi, A. S., & Conte, R. (2022). Separation and evaluation of potential antioxidant, analgesic, and anti-inflammatory activities of limonene-rich essential oils from *Citrus sinensis* (L.). *Open Chemistry*, 20(1), 1517-1530.
7. Wang, X., Li, G., & Shen, W. (2018). Protective effects of D-limonene against transient cerebral ischemia in stroke-prone spontaneously hypertensive rats. *Experimental and Therapeutic Medicine*, 15(1), 699-706.
8. Wald, A., & Johnston, C. (2021). Treatment and prevention of herpes simplex virus type 1 in immunocompetent adolescents and adults. Retrieved February 26.
9. De Clercq, E. (2004). Antiviral drugs in current clinical use. *Journal of Clinical Virology*, 30(2), 115-133.
10. Farahpour, M. R., & Habibi, M. (2012). Evaluation of the wound healing activity of an ethanolic extract of Ceylon cinnamon in mice. *Veterinary Medicine*, 57(1), 53-57.
11. Nayak, B. S., Raju, S. S., Eversley, M., & Ramsubhag, A. (2009). Evaluation of wound healing activity of *Lantana camara* L.–a preclinical study. *Phytotherapy Research*, 23(2), 241-245.
12. Zhang, X., Lin, C., Lu, A., Lin, G., Chen, H., Liu, Q., & Zhang, H. (2017). Liposomes equipped with cell-penetrating peptide BR2 enhance the chemotherapeutic effects of cantharidin against hepatocellular carcinoma. *Drug Delivery*, 24(1), 986-998.
13. Ahmed, H. A., Salama, Z. A., Salem, S. H., Aly, H. F., Nassrallah, A., Abou-Elella, F., & Aboul-Enein, A. M. (2021). Lycopene nanoparticles ameliorate the antioxidants, antimicrobial, and anticancer potencies

of tomato pomace. *Egyptian Journal of Chemistry*, 64(7), 3739-3749.
14. Al-Abboodi, A., Alsaady, H. A., Banoon, S. R., & Al-Saady, M. (2021). Conjugation strategies on functionalized iron oxide nanoparticles as a malaria vaccine delivery system. *Bionatura*, 3(3), 2009-2016.
15. Al-Abboodi, A., Albukhaty, S., Sulaiman, G. M., Al-Saady, M. A., Jabir, M. S., & Abomughaid, M. M. (2024). Protein-conjugated superparamagnetic iron oxide nanoparticles for efficient vaccine delivery systems. *Plasmonics*, 19(1), 379-388.
16. Hassan, S. A., Almaliki, M. N., Hussein, Z. A., Albehadili, H. M., Banoon, S. R., Al-Abboodi, A., & Al-Saady, M. (2023). Development of nanotechnology by artificial intelligence: A comprehensive review. *Journal of Nanostructures*, 13(4), 915-932.
17. Singh, S. D. J., Krishna, V., Mankani, K. L., Manjunatha, B. K., Vidya, S. M., & Manohara, Y. N. (2005). Wound healing activity of the leaf extracts and deoxyelephantopin isolated from *Elephantopus scaber* Linn. *Indian Journal of Pharmacology*, 37(4), 238.
18. Simões, C. M. O., Amoros, M., & Girre, L. (1999). Mechanism of antiviral activity of triterpenoid saponins. *Phytotherapy Research*, 13(4), 323-328.
19. Tang, W., Zhang, Z., Nie, D., Li, Y., Liu, S., & Li, Y. (2023). Protective effect of *Citrus medica limonum* essential oil against *Escherichia coli* K99-induced intestinal barrier injury in mice. *Nutrients*, 15(12), 2697.
20. Schmidtke, M., Knorre, C., Blei, L., Stelzner, A., & Birch-Hirschfeld, E. (1998). Penetration and antiviral activity of Coxsackievirus B3 (CVB3)-specific phosphorothioate oligodeoxynucleotides (PS-ODN). *Nucleosides and Nucleotides*, 17(9-11), 1557-1566.
21. Ahmed, H. A., Aboul-Enein, A. M., Abou-Elella, F., Salem, S. H. E., Aly, H. F., Nassrallah, A., & Salama, Z. (2021). Nano-formulations of hesperidin and essential oil extracted from sweet orange peel: Chemical properties and biological activities. *Egyptian Journal of Chemistry*, 64(9), 5373-5385.
22. Zhao, C., Zhang, Z., Nie, D., & Li, Y. (2022). Protective effect of lemon essential oil and its major active component, D-limonene, on intestinal injury and inflammation of *E. coli*-challenged mice. *Frontiers in Nutrition*, 9, 843096.
23. Espinosa-Andrews, H., Sandoval-Castilla, O., Vázquez-Torres, H., Vernon-Carter, E. J., & Lobato-Calleros, C. (2010). Determination of the gum Arabic–chitosan interactions by Fourier Transform Infrared Spectroscopy and characterization of the microstructure and rheological features of their coacervates. *Carbohydrate Polymers*, 79(3), 541-546.
24. Hasanien, Y. A., Nassrallah, A. A., Zaki, A. G., & Abdelaziz, G. (2022). Optimization, purification, and structure elucidation of anthraquinone pigment derivative from *Talaromyces purpureogenus* as a novel promising antioxidant, anticancer, and kidney radio-imaging agent. *Journal of Biotechnology*, 356, 30-41.
25. Badawy, M. E., Saad, A. F. S., Tayeb, E. S. H., Mohammed, S. A., & Abd-Elnabi, A. D. (2017). Optimization and characterization of the formation of oil-in-water diazinon nanoemulsions: Modeling and influence of the oil phase, surfactant, and sonication. *Journal of Environmental Science and Health, Part B*, 52(12), 896-911.
26. Gurtner, G., Werner, S., Barrandon, Y., & Longaker, M. (2008). Wound repair and regeneration. *Nature*, 453, 314–321.
27. AbouAitah, K., Soliman, A. A., Swiderska-Sroda, A., Nassrallah, A., Smalc-Koziorowska, J., Gierlotka, S., & Lojkowski, W. (2022). Co-delivery system of curcumin and colchicine using functionalized mesoporous silica nanoparticles promotes anticancer and apoptosis effects. *Pharmaceutics*, 14(12), 2770.
28. Abouelenein, M. G., El-Rashedy, A. A., Awad, H. M., El Farargy, A. F., Nassar, I. F., & Nassrallah, A. (2023). Synthesis, molecular modeling insights, and anticancer assessment of novel polyfunctionalized pyridine congeners. *Bioorganic Chemistry*, 141, 106910.
29. Dwivedi, D., Dwivedi, M., Malviya, S., & Singh, V. (2017). Evaluation of wound healing, anti-microbial and antioxidant potential of *Pongamia pinnata* in Wistar rats. *Journal of Traditional and Complementary Medicine*, 7(1), 79–85.
30. Salamatullah, A. M., Subash-Babu, P., Nassrallah, A., Alshatwi, A. A., & Alkaltham, M. S. (2021). Cyclotrisiloxan and β-sitosterol-rich *Cassia alata* (L.) flower inhibit HT-115 human colon cancer cell growth via mitochondrial-dependent apoptotic stimulation. *Saudi Journal of Biological Sciences*, 28(10), 6009-6016.
31. Marônek, M., Marafini, I., Gardlík, R., Link, R., Troncone, E., & Monteleone, G. (2021). Metalloproteinases in inflammatory bowel diseases. *Journal of Inflammation Research*, 14, 1029–1041.
32. Atkinson, J. J., Toennies, H. M., Holmbeck, K., & Senior, R. M. (2007). Membrane type 1 matrix metalloproteinase is necessary for distal airway epithelial repair and keratinocyte growth factor receptor expression after acute injury. *American Journal of Physiology - Lung Cellular and Molecular Physiology*, 293, L600–L610.
33. Cos, P., Vlietinck, A. J., Berghe, D. V., Maes, L., De Logu, A., Loy, G., Pellerano, M. L., Bonsignore, L., & Schivo, M. L. (2000). Inactivation of HSV-1 and HSV-2 and prevention of cell-to-cell virus spread by *Santolina insularis* essential oil. *Antiviral Research*, 48, 177–185.
34. Eerola, L. M., Alho, H. S., Maasilta, P. K., Inkinen, K. A., Harjula, A. L., Litmanen, S. H., & Salminen, U. S. (2005). Matrix metalloproteinase induction in post-transplant obliterative bronchiolitis. *The Journal of Heart and Lung Transplantation*, 24(4), 426-432.
35. Astani, A., Reichling, J., & Schnitzler, P. (2010). Comparative study on the antiviral activity of selected monoterpenes derived from essential oils. *Phytotherapy Research*, 24, 673–679.
36. Tragoolpua, Y., & Jatisatieur, A. (2007). Anti-herpes simplex virus activities of *Eugenia caryophyllus* (Spreng.) Bullock & S. G. Harrison and essential oil, eugenol. *Phytotherapy Research*, 21, 1153–1158.